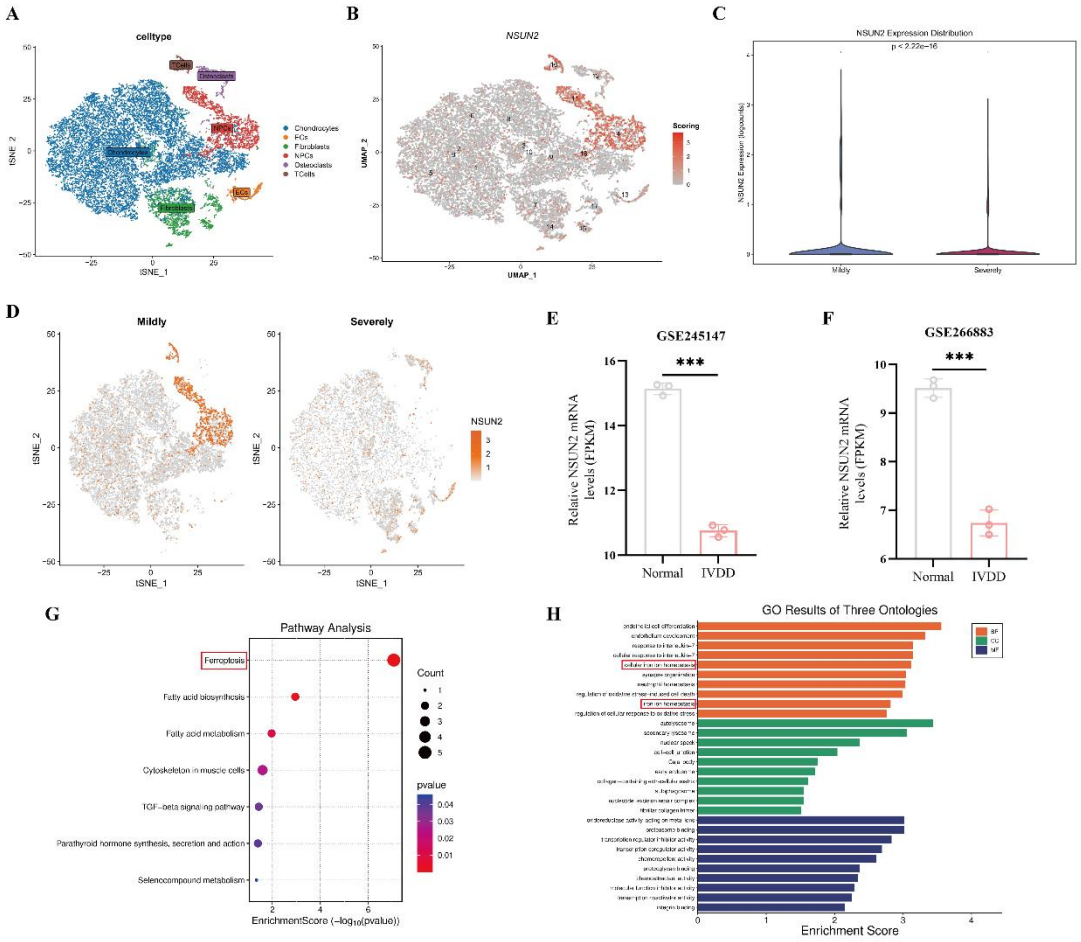

Figure S1. Integration of single-cell and bulk RNA sequencing data revealed that NSUN2 expression is significantly decreased in degenerating NP tissue. (A) UMAP visualizing human NPCs as six different clusters within human NP tissue after unsupervised clustering (n = 3). (B) NSUN2 is predominantly expressed in NPCs. (C, D) NSUN2 expression gradually decreased with the progression of intervertebral disc degeneration. (E, F) Bulk RNA sequencing reveals the relative fold change of NSUN2 expression in normal and IVDD tissues (n = 3). (G) KEGG analysis of top 30 genes exhibiting the highest correlation with NSUN2 based on single- cell sequencing data, revealing that NSUN2 may be implicated in ferroptosis of NPCs. (h) GO enrichment analysis suggested that NSUN2 might be linked to intracellular iron homeostasis in NPCs. Data are presented as the mean ± SD. ***p < 0.001.

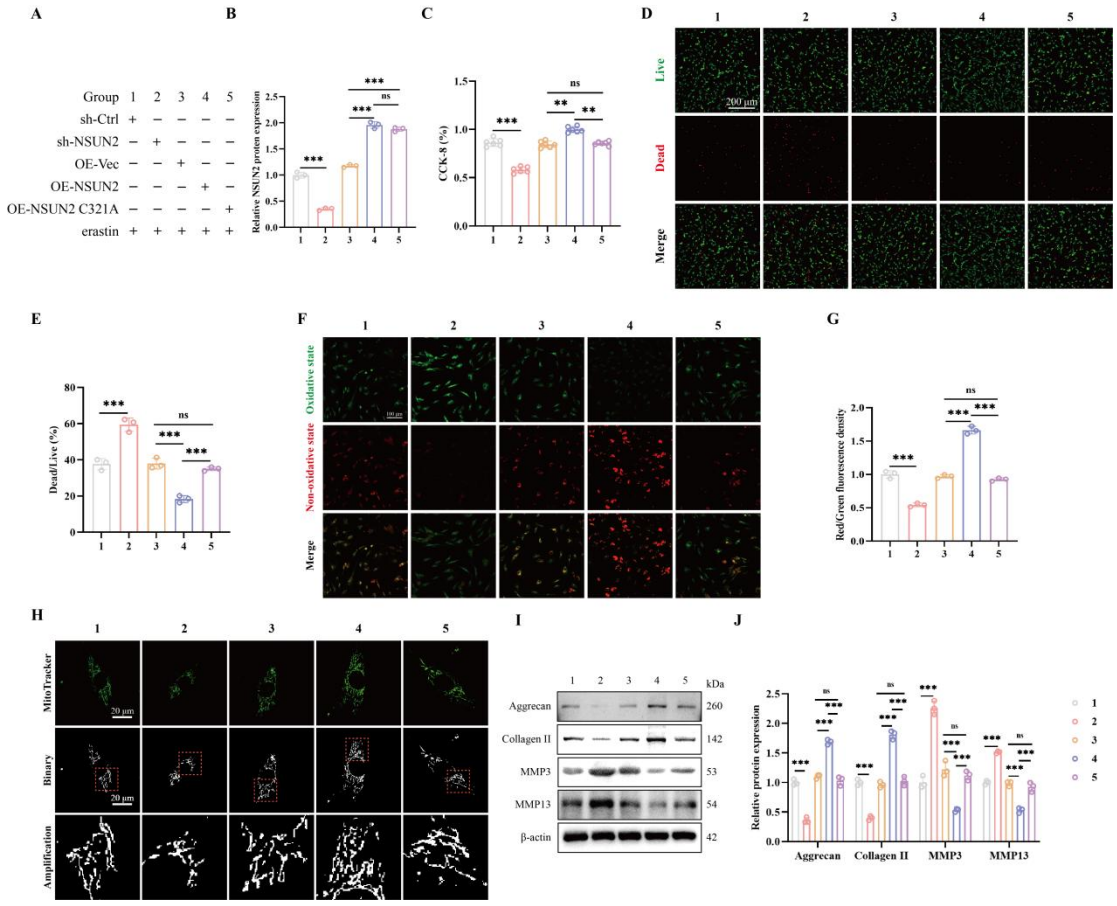

Figure S2. Knockdown of NSUN2 promotes NPCs ferroptosis *in vitro*. (A) Experimental assignment. (B) Quantitative assessment the transfection efficiency (n = 3). (C) CCK-8 assay to assess NPCs viability in NSUN2 knockdown or NSUN2 overexpression conditions (n = 6). (D, E) Calcein-AM/PI staining to evaluate NPCs viability in NSUN2 knockdown or NSUN2 overexpression conditions (scale bar: 200μm; n = 3). (F, G) Quantitative assessment of lipid peroxidation levels in NPCs using BODIPY 581/591 C11 fluorescence staining (scale bar: 100μm; n = 3). (H) Mitochondrial morphology in NPCs was observed using MitoTracker Green staining (scale bar: 20μm). (I, J) Western blot analysis of IVDD-related indicators and quantified using Image J (n = 3). Data are presented as the mean ± SD. **p < 0.01, ***p < 0.001; ns, not significant.

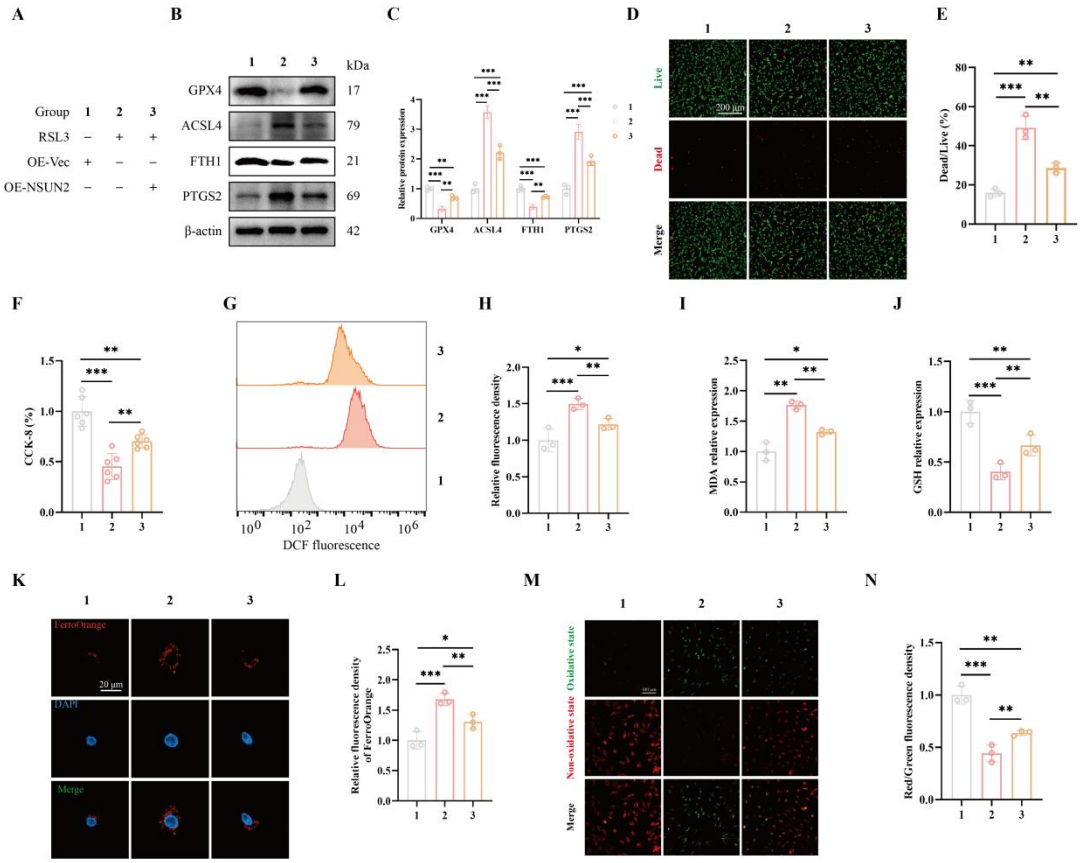

Figure S3. Overexpression of NSUN2 alleviates RSL3-induced ferroptosis. (A)Experimental groups. (B, C) Ferroptosis-related marker protein levels between groups (n = 3). (D, E) Calcein-AM/PI staining to evaluate NPCs viability (scale bar: 200μm; n = 3). (F) CCK-8 assay to assess NPCs viability (n = 6). (G-J) ROS, GSH and MDA concentrations were measured (n = 3). (K, L) Detection and quantification of intracellular Fe^{2+} using FerroOrange staining (scale bar: 20μm; n = 3). (M, N) Quantitative assessment of lipid peroxidation levels in NPCs using BODIPY 581/591 C11 fluorescence staining (scale bar: 100μm; n = 3). *p < 0.05, **p < 0.01, ***p < 0.001.

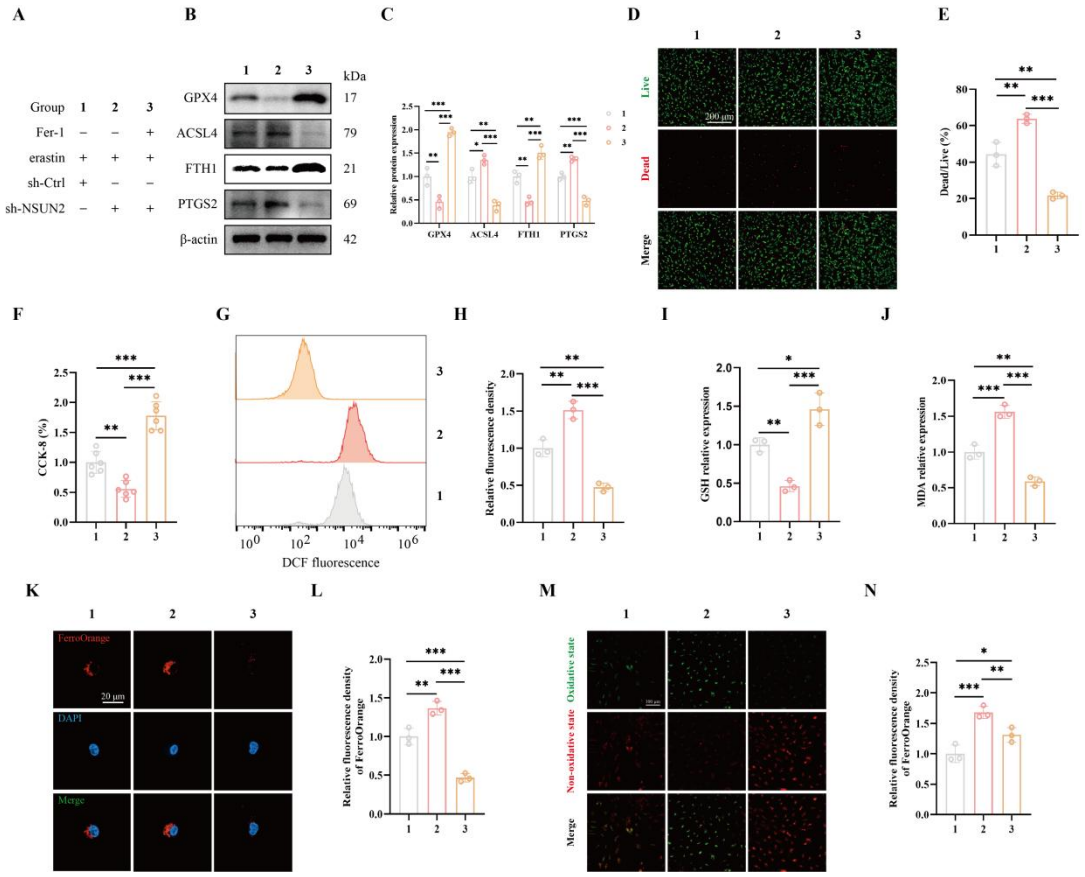

Figure S4. Ferrostatin-1 ameliorates knockdown of NSUN2-induced ferroptosis. (A)Experimental groups. (B, C) Ferroptosis-related marker protein levels between groups (n = 3). (D, E) Calcein-AM/PI staining to evaluate NPCs viability (scale bar: 200μm; n = 3). (F) CCK-8 assay to assess NPCs viability (n = 6). (G-J) ROS, GSH and MDA concentrations were measured (n = 3). (K, L) Detection and quantification of intracellular Fe^{2+} using FerroOrange staining (scale bar: 20μm; n = 3). (M, N) Quantitative assessment of lipid peroxidation levels in NPCs using BODIPY 581/591 C11 fluorescence staining (scale bar: 100μm; n = 3). *p < 0.05, **p < 0.01, ***p < 0.001.

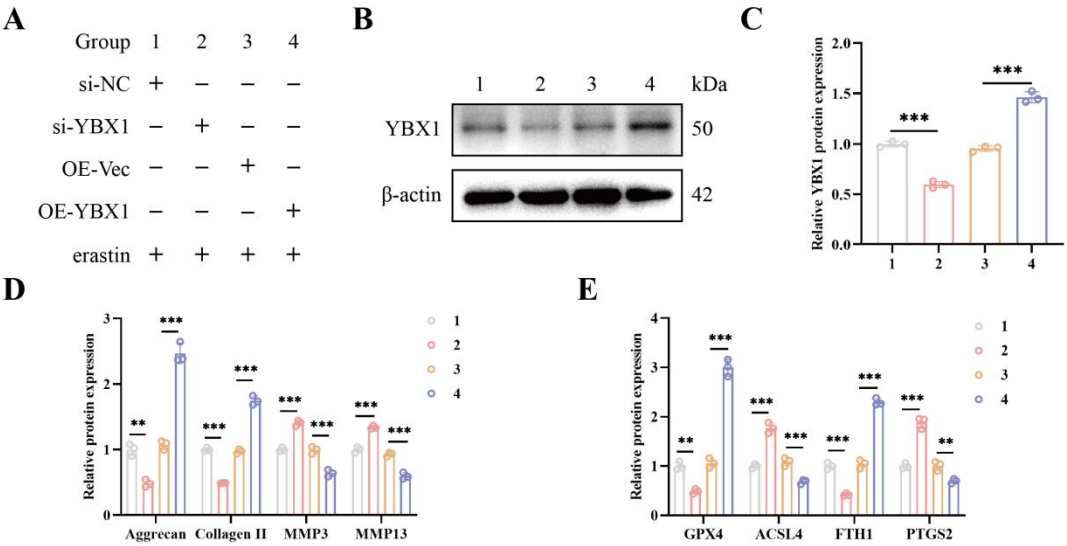

Figure S5. YBX1 recognizes m5C modification of *Fth1* and stabilizes *Fth1* mRNA. (A) Experimental assignment. (B, C) The transfection efficiency was confirmed by western blot analysis and quantified using Image J (n = 3). (D) Quantitative assessment of IVDD-related indicators in NPCs after treatment with si-YBX1 or OE-YBX1 (n = 3). (E) Quantitative assessment of ferroptosis-related indicators in NPCs after treatment with si-YBX1 or OE-YBX1 (n = 3). Data are presented as the mean ± SD. **p < 0.01, ***p < 0.001.

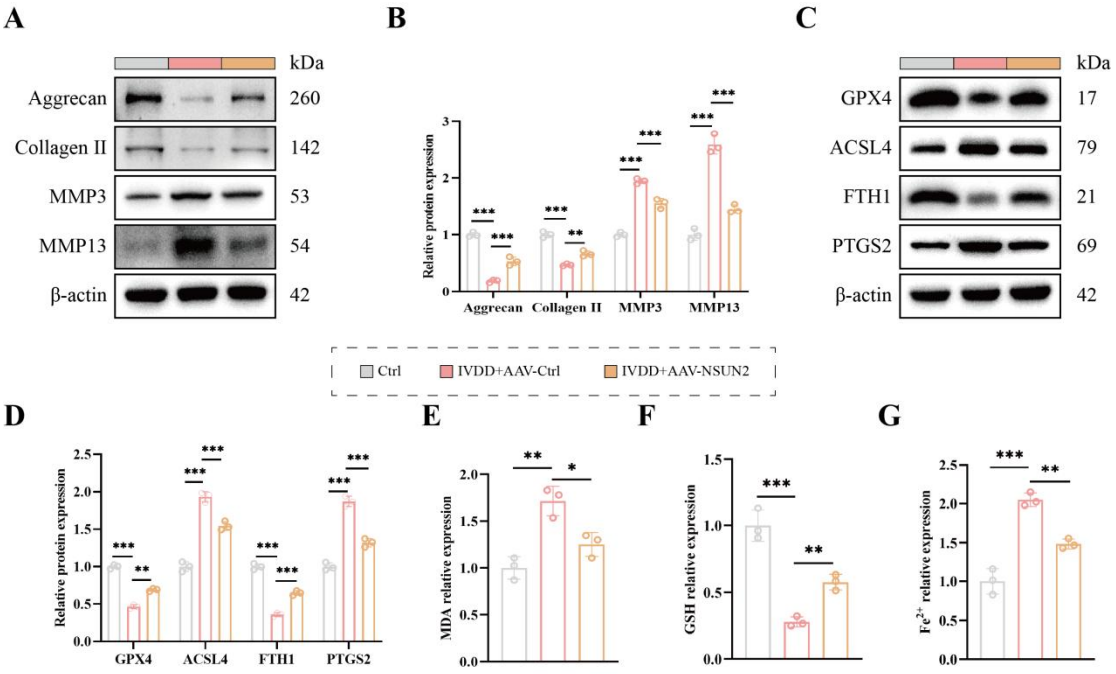

Figure S6. Overexpression of NSUN2 mitigates rat IVDD. (A, B) Representative western blots showing expression levels of IVDD-related indicators in rat treated with

AAV-Ctrl or AAV-NSUN2 (n = 3). (C, D) Representative western blots showing expression levels of ferroptosis-related indicators in rat treated with AAV-Ctrl or AAV-NSUN2 (n = 3). (E-G) Quantification of MDA, GSH, and Fe^{2+} concentrations in rat treated with AAV-Ctrl or AAV-NSUN2 (n = 3). Data are presented as the mean ± SD. *p < 0.05, **p < 0.01, ***p < 0.001.

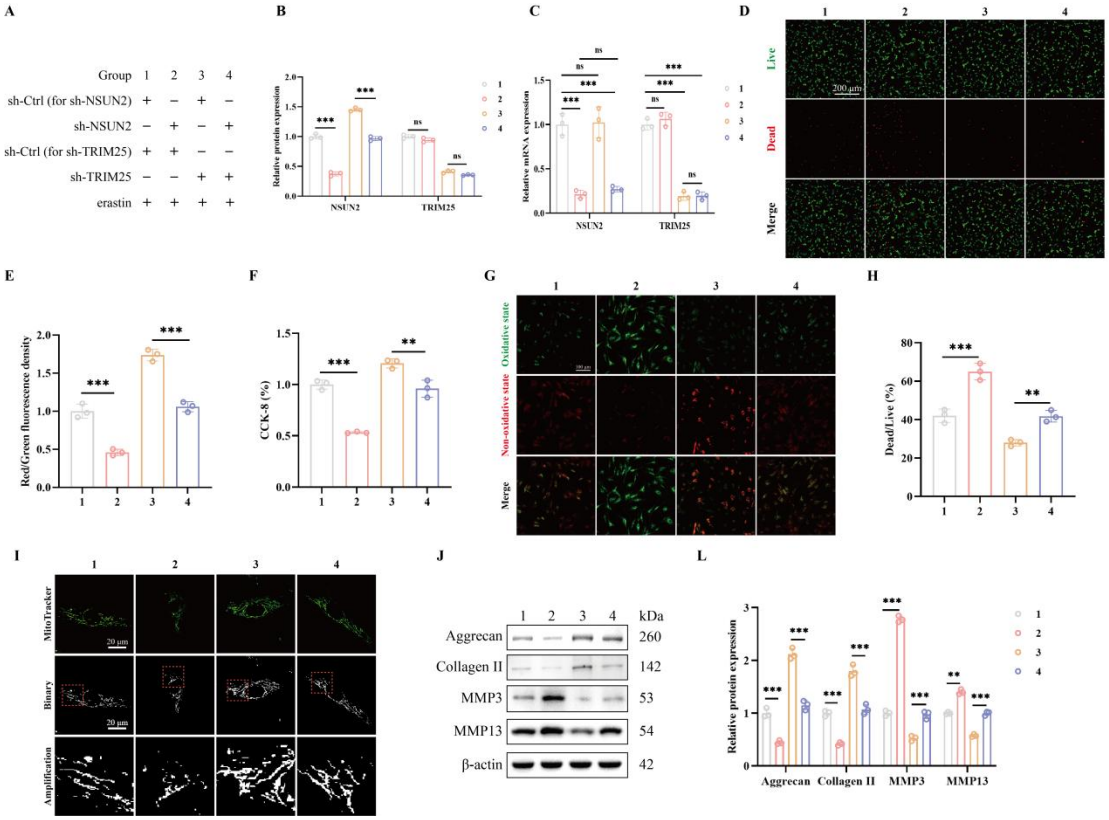

Figure S7. Knockdown of TRIM25 attenuates ferroptosis induced by NSUN2 deficiency in NPCs. (A) Experimental assignment. (B, C) Quantitative assessment the transfection efficiency (n = 3). (D, E) Calcein-AM/PI staining to evaluate NPCs viability in TRIM25 knockdown or NSUN2 knockdown conditions (scale bar: 200μm; n = 3). (F) CCK-8 assay to assess NPCs viability in TRIM25 knockdown or NSUN2 knockdown conditions (n = 6). (G, H) Quantitative assessment of lipid peroxidation levels in NPCs using BODIPY 581/591 C11 fluorescence staining (scale bar: 100μm; n = 3). (I) Mitochondrial morphology in NPCs was observed using MitoTracker Green staining (scale bar: 20μm). (J, K) Western blot analysis of IVDD-related indicators and quantified using Image J (n = 3). Data are presented as the mean ± SD. **p < 0.01, ***p < 0.001; ns, not significant.

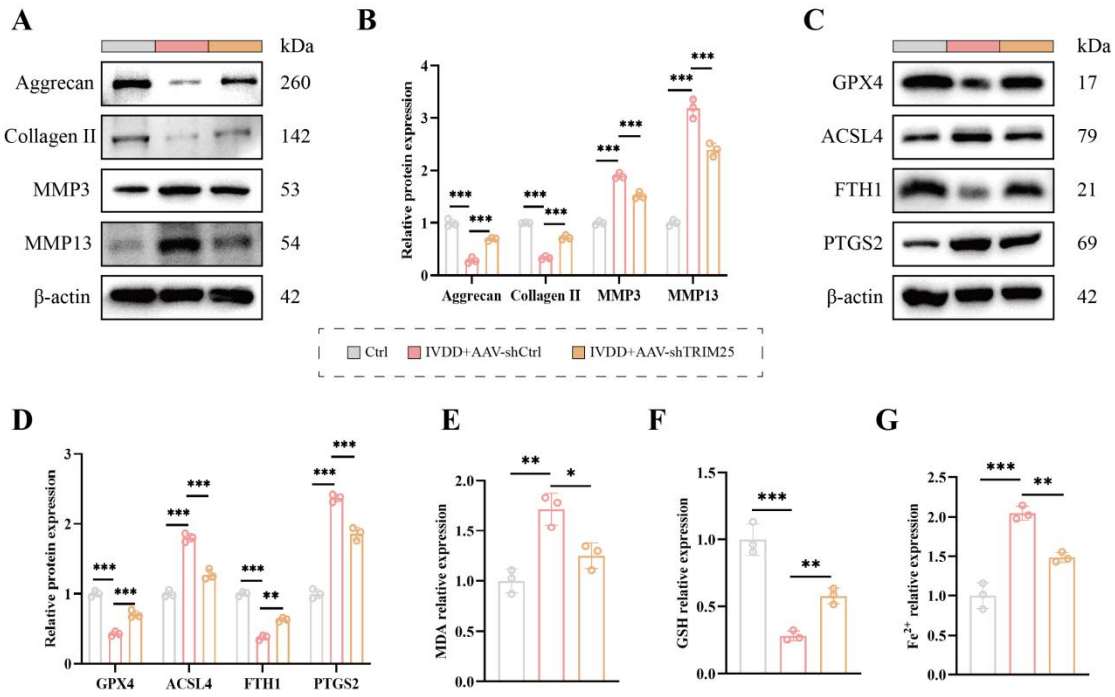

Figure S8. Knockdown of TRIM25 ameliorates rat IVDD. (A, B) Representative western blots showing expression levels of IVDD-related indicators in rat treated with AAV-shCtrl or AAV-shTRIM25 (n = 3). (C, D) Representative western blots showing expression levels of ferroptosis-related indicators in rat treated with AAV-shCtrl or AAV-shTRIM25 (n = 3). (E-G) Quantification of MDA, GSH, and Fe^{2+} concentrations in rat treated with AAV-shCtrl or AAV-shTRIM25 (n = 3). Data are presented as the mean ± SD. *p < 0.05, **p < 0.01, ***p < 0.001.

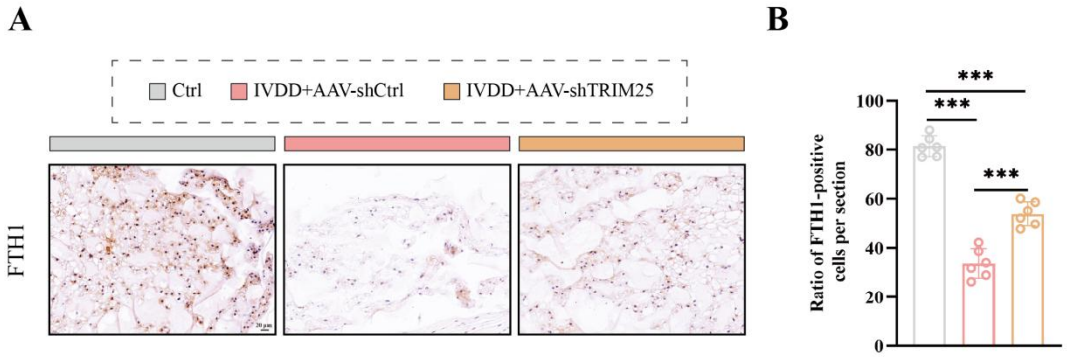

Figure S9. Knockdown of TRIM25 partially restores FTH1 expression levels in rat intervertebral disc tissues. (A, B) Immunohistochemical staining and quantitative analysis of FTH1 in rat intervertebral discs (scale bar: 20μm; n = 3). ***p < 0.001.

Supplementary Table 1. The primer sequences used for RT-qPCR.

Target	Forward	Reverse
FTH1	ACTACCACCAGGACTCAGAGG	AGTCATCACAGTCTGGTTTCTTGA
YBX1	GACAAAAGCAGCCGATCCAC	TGTTGGATGACTAAACCGGATG
GPX4	TTGGTCGGCTGGACGAGG	GGGACGCGCACATGGT
SLC7A11	TGTGTGGGGTCCTGTCACTA	CAGTAGCTGCAGGGCGTATT
ACSL4	AAGTAGACCAACGCCTTCA	CAGTCCAGGTATTCTTTCACA
PTGS2	CTGGGAGCCACCTGTTACTG	CGGCTGTGCATCATACAACG
TFRC	GTTGCAGCCTTACTATACGCC	GCAGCACGTCGCTTATATTGG
SLC3A2	ACCCCTGTTTTCAGCTACGG	GGTCTTCACTCTGGCCCTTC
SAT1	CCTGACTGAGAAGAGGACGC	TTCATATTTAGCCAGCTCCTTGA

Supplementary Table 2. The primary antibodies used for immunoblotting or immunofluorescence.

Target	Source	Catalog number	Dilution ratio
NSUN2	Proteintech	20854-1-AP	WB 1:5000 IF 1:1500
m5C	Proteintech	68301-1-Ig	WB 1:3000
Aggrecan	Affinity	DF7561	WB 1:1000
Collagen II	Servicebio	GB11021-100	WB 1:500
MMP3	Affinity	AF0217	WB 1:1000
MMP13	Affinity	AF5355	WB 1:1000
GPX4	Proteintech	67763-1-Ig	WB 1:1000
ACSL4	Affinity	DF12141	WB 1:500
FTH1	Affinity	DF6278	WB 1:1000
PTGS2	Affinity	AF7003	WB 1:1000
YBX1	Proteintech	20339-1-AP	WB 1:5000
TRIM25	Proteintech	12573-1-AP	WB 1:5000
Flag-Tag	Proteintech	20543-1-AP	WB 1:20000
HA-Tag	Proteintech	51064-2-AP	WB 1:5000
Myc-Tag	Proteintech	60003-2-Ig	WB 1:5000
Ub	Proteintech	10201-2-AP	WB 1:1000
β-actin	Proteintech	66009-1-Ig	WB 1:20000